ACS APPLIED MATERIALS & INTERFACES

Research Article

www.acsami.org

Bioinspired Formation of 3D Hierarchical $CoFe_2O_4$ Porous Microspheres for Magnetic-Controlled Drug Release

Bin Cai,[†] Minggang Zhao,[†] Ye Ma,[†] Zhizhen Ye,[†,‡] and Jingyun Huang*[,†,‡]

[†]Department of Materials Science and Engineering, State Key Laboratory of Silicon Materials, and [‡]Cyrus Tang Center for Sensor Materials and Applications, Zhejiang University, Hangzhou 310027, China

Supporting Information

ABSTRACT: Bioinspired by the morphology of dandelion pollen grains, we successfully prepared a template-free solution-based method for the large-scale preparation of three-dimensional (3D) hierarchical $CoFe_2O_4$ porous microspheres. Besides, on the basis of the effect of the reaction time on the morphology evolution of the precursor, we proposed an in situ dissolution−recrystallization growth mechanism with morphology and phase change to understand the formation of dandelion pollenlike microspheres. Doxorubicin hydrochloride, an anticancer drug, is efficiently loaded into the $CoFe_2O_4$ microspheres. The magnetic nanoparticles as field-controlled drug carriers offer a unique power of magnetic guidance and field-triggered drug-release behavior. Therefore, 3D hierarchical $CoFe_2O_4$ porous microspheres demonstrate the great potential for drug encapsulation and controlled drug-release applications.

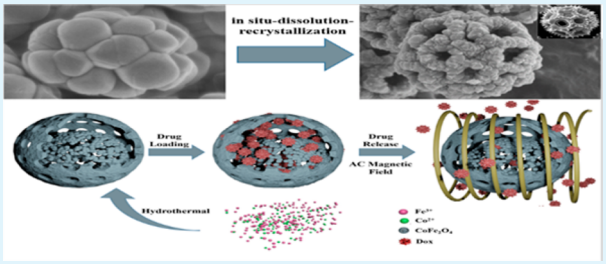

KEYWORDS: *$CoFe_2O_4$, bioinspired, microsphere, controlled release*

1. INTRODUCTION

In the last several years, advanced nanoscale systems for remotely controlled drug release have received tremendous attention, in particular from the field of nanomedicine.[1] The drug carriers with targeted-delivery capability and controlled release behavior can remarkably improve the therapeutic efficiency and greatly minimize side effects.[2] Currently, sustained and controlled drug release can be achieved by thermo-,[3] pH-,[4] light-,[5] ultrasound-,[6] or magnetic-sensitive[7] nanoparticle systems. Among these, magnetically responsive systems can be a magnetic guidance in the permanent magnetic field, so the drug can be targeted delivered. Additionally, a temperature increase can lead to controlled drug release when an alternating-current magnetic field (AMF) is applied. Therefore, a magnetically responsive system is a good choice for the drug carrier. However, most magnetically responsive systems are based on magnetic nanoparticles encapsulated with hollow mesoporous silica shells that will largely reduce the magnetization saturation.[8−10] Also, traditional magnetically responsive systems always need a high-frequency AMF and consume a great amount of power.[11] Therefore, it is necessary to set up a magnetically responsive system with high magnetization saturation and that can realize high-efficacy externally controlled drug release under a remote low-energy AMF.

In order to effectively encapsulate drug and controlled release of the loading drug in the presence of an external magnetic field, it is necessary to design a porous composite magnetic drug carrier. In this respect, cobalt ferrite ($CoFe_2O_4$) nanomaterials are excellent candidates for cancer therapy. $CoFe_2O_4$ nanomaterials exhibit high saturation magnetization, coercivity, and specific surface areas,[12] which lead to wide applications in drug delivery,[13] magnetic response imaging,[14] and magnetic storage.[15] $CoFe_2O_4$ have been prepared by diverse methods, such as combustion reaction, coprecipitation, and hydrothermal and sol−gel synthesis.[16−19] However, most of $CoFe_2O_4$ prepared by these methods are simply nanoparticles without any hierarchical structures, which are not proper for drug loading and release. It is necessary to design a plan to prepare suitable $CoFe_2O_4$ nanomaterials. In reality, nature is seen to be the most superior master in creating amazing hierarchical structures. It can provide us with lots of inspiration for the design of functional materials. In particular, pollen grains, the male gametophytes of higher plants, contain special kinds of porous hierarchical structures.[20−24] The open porous supporting scaffold of a pollen grain provides a large surface area for biomolecule loading and facilitates the diffusion of chemicals into the grain. Such an architecture is also desirable in a controlled drug-carrier system. Bioinspired by this, we think that it would be promising to mimic the specific construction of pollen grains to enhance the performances of $CoFe_2O_4$ nanomaterials.

In this work, we have devised a template-free solution-based method for the preparation of a new type of dandelion pollenlike $CoFe_2O_4$ nanostructure. To the best of our knowledge, only a few researches have reported the preparation

Received: November 4, 2014
Accepted: December 25, 2014
Published: December 25, 2014

DOI: 10.1021/am507689a
ACS Appl. Mater. Interfaces 2015, 7, 1327−1333

Scheme 1. Schematic Illustration of the Drug Loading and Release Behaviors of the Magnetically Responsive System

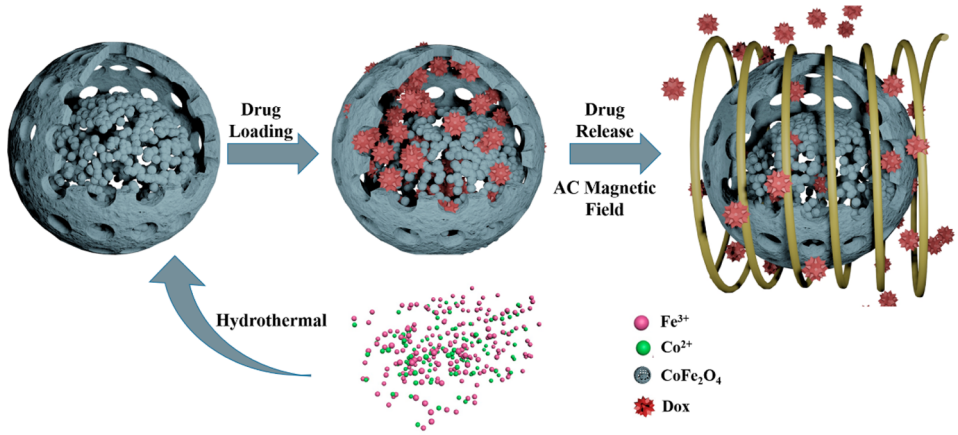

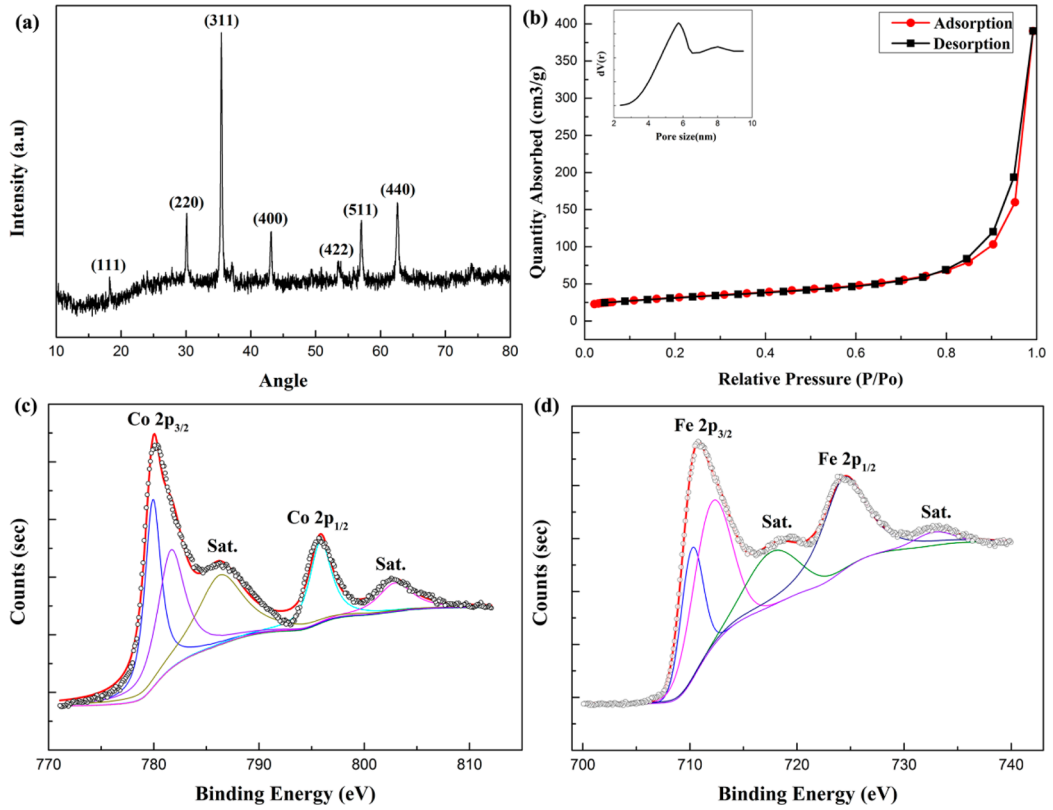

Figure 1. XRD pattern of the obtained $CoFe_2O_4$ microspheres (a). N_2 adsorption−desorption isotherms of $CoFe_2O_4$ microspheres (b). XPS spectra of the Co 2p (c) and Fe 2p (d) regions of the $CoFe_2O_4$ microspheres.

of three-dimensional (3D) hierarchical $CoFe_2O_4$ porous microspheres. More importantly, on the basis of the effect of investigation of the reaction time on the morphology evolution of the precursor, we proposed an in situ dissolution−recrystallization growth mechanism accompanied by morphology and phase change to understand the formation of 3D porous microspheres. The mechanism provides a new research opportunity for investigating the formation of novel micro/nanostructures. The as-synthesized $CoFe_2O_4$ microspheres show excellent magnetic performance, which suggests good magnetic guidance capability of the designed drug carrier. Furthermore, we discussed the remotely controlled drug-release behavior under an AMF with different frequencies and strengths. It is observed that the AMF can efficiently control the drug release. Therefore, the synthesized dandelion pollenlike $CoFe_2O_4$ microspheres prove to be promising materials for drug encapsulation and controlled drug-release applications.

2. EXPERIMENTAL SECTION

2.1. Synthesis of Dandelion Pollenlike $CoFe_2O_4$ Microspheres. All chemicals used in this work were of analytical grade and were used as received without further purification. In a typical synthesis, 8 mM ferric nitrate nonahydrate $[Fe(NO_3)_3{\cdot}9H_2O]$, 4 mM cobalt acetate tetrahydrate $[Co(Ac)_2{\cdot}4H_2O]$, 80 mM urea, and 120 mM ammonium fluoride (NH_4F) were dissolved in 30 mL of deionized water (18.2 MΩ·cm resistivity) under stirring at room temperature. After stirring for 10 min, 0.1 M nitric acid (HNO_3) was added dropwise to the solution until the pH was adjusted to 5.0. The

DOI: 10.1021/am507689a
ACS Appl. Mater. Interfaces 2015, 7, 1327−1333

homogeneous solution was subsequently transferred into a 50 mL Teflon-lined stainless steel autoclave. The autoclave was sealed and maintained at 180 °C for 20 h in an electric oven. After cooling to room temperature naturally, the precipitate was collected and rinsed with deionized water and ethanol several times before it was dried in a vacuum oven at 60 °C for 6 h.

2.2. Drug Loading and Release. The drug loading and release behaviors of the magnetically responsive system are illustrated in Scheme 1. Doxorubicin hydrochloride (DOX), a common anticancer drug, was chosen as a model drug to investigate the loading capacity, encapsulation efficiency, and in vitro release rate. Briefly, the obtained $CoFe_2O_4$ hollow porous microspheres (28.5 mg) were mixed with a DOX (3.8 mg) solution in phosphate-buffered saline (PBS). After stirring for 24 h under dark conditions, the DOX-loaded nanoparticles were centrifuged at 10000 rpm for 5 min and washed with PBS two times in order to remove free DOX molecules. The loading capacity and efficiency were evaluated by measuring the relative intensity of the UV−vis absorption of the standard DOX solution and supernatant at 480 nm, respectively.

For the drug-release experiment, the obtained $CoFe_2O_4$ hollow porous microspheres (15 mg) were mixed with a DOX (20 mL of 0.2 mg/mL) solution in PBS. After stirring for 24 h under dark conditions, the DOX-loaded nanoparticles were centrifuged at 10000 rpm for 5 min and washed with PBS two times in order to remove free DOX molecules. The DOX-loaded nanoparticles were dispersed in 20 mL of a pH 7.4 or pH 5 buffer solution at room temperature. The release system was centrifuged every 1 h at 10000 rpm for 3 min. Then, 4 mL of the supernatant was removed, and the concentration of DOX released in solution was evaluated by UV−vis absorption spectroscopy. Fresh buffer (4 mL) replaced the removed supernatant, and the solution was subjected to drug release again. To exploit the potential of magnetic-controlled drug release, $CoFe_2O_4$ microspheres loaded with DOX drug were exposed to an external magnetic field with different frequencies (0, 50, 60, 70, 100, 200, and 400 Hz) and strengths (current intensities of 3, 6, and 9 A). According to the electromagnetic induction theory, the higher the current intensity, the larger the magnetic field strength). The same process was adopted to determine the release behavior of the magnetic-stimulated system.

2.3. Materials Characterization. The morphology of the samples was characterized by field-emission scanning electron microscopy (FESEM; Hitachi S-4800) and transmission electron microscopy (TEM; Tecnai F20). The crystal phase of the products was examined by X-ray diffraction (XRD; Cu Kα, λ = 1.5406 Å) over the 2θ range of 10−80°. Specific surface areas were calculated from the results of N_2 adsorption−desorption isotherms at 77 K (Quantachrome ASIC-2) by using the Brunauer−Emmet−Teller (BET) method. X-ray photoelectron spectroscopy (XPS; Escalab 250Xi) measurements were performed with a monochromatic Al Kα ($h\nu$ = 1486.6 eV) X-ray source. Magnetic measurements were carried out with a superconducting quantum interference device (SQUID) magnetometer (MPMS-XL-5) at room temperature. UV−vis absorption measurements were carried out with a Shimadzu UV3600 spectrophotometer.

3. RESULTS AND DISCUSSION

3.1. Synthesis and Characterization. XRD measurement was used to investigate the phase and structure of the synthesized samples. As shown in Figure 1a, all diffraction peaks of the XRD pattern can be assigned to a single phase of $CoFe_2O_4$ with a face-centered-cubic spinel structure (JCPDS no. 22-1086). Figure 1c shows the XPS spectra of Co 2p in $CoFe_2O_4$ in the binding energy between 770 and 810 eV. It shows that Co $2p_{3/2}$ is composed of two main doublets with peak positions at 779.9 and 781.6 eV, associated with a corresponding satellite at 786.3 eV. The peak of Co $2p_{1/2}$ is located at 795.8 eV with a corresponding satellite at 802.9 eV. The intense satellite structure is attributed to the spin−orbit splitting of Co 2p photoelectron lines.[25] Figure 1d shows a Fe 2p photoionization region between 700 and 740 eV. It yields Fe $2p_{3/2}$ binding energies of 710.2 and 712.1 eV and a Fe $2p_{1/2}$ binding energy of 724.4 eV, which is consistent with the Fe 2p binding energy for $CoFe_2O_4$ microspheres.[26,27] N_2 sorption isotherms were provided to investigate the BET surface areas of the $CoFe_2O_4$ porous microspheres, and the data are presented in Figure 1b. The isotherm of the $CoFe_2O_4$ microspheres can be classified as type IV with a type H1 hysteresis loop, determining this structure to be mesoporous. The BET surface areas and pore volumes of the samples are as high as 111.57 m^2/g and 0.604 cm^3/g, respectively, which are relatively large values for magnetic nanocomposites.[28−30] Except for the open pores' networks on the shells, the corresponding mesopore size distribution calculated from the desorption branch of the N_2 isotherms is narrow, peaking at 4−8 nm (Figure 1b). It can supply large areas for drug encapsulation.

The morphology of the $CoFe_2O_4$ porous microspheres was analyzed by FESEM. As shown in Figure 2a−c, the hierarchical

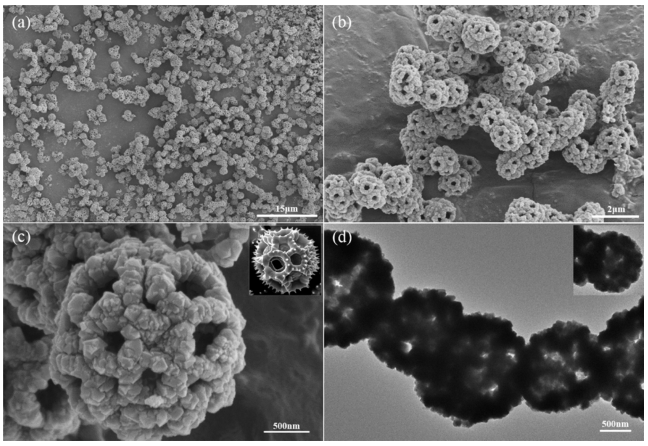

Figure 2. SEM images of the $CoFe_2O_4$ porous microspheres: (a and b) low-magnification SEM images; (c) high-magnification SEM image of the individual $CoFe_2O_4$ microspheres. Inset: morphology of dandelion pollen grains. (d) TEM image of the $CoFe_2O_4$ microspheres.

scaffolds of a dandelion pollen grain (inset picture of Figure 2c) are mainly mimicked by the obtained $CoFe_2O_4$ microsphere. The microsphere is about 1 μm in diameter. The open pores' networks on the shells are similar to those of dandelion pollen grains. The pore size is around 100−200 nm. It also can be revealed that the structure is highly porous and composed of nanosized building blocks (Figure 2c). The TEM image shown in Figure 2d gives further characterization of the sample. The feature structure of the sample is inconsistent with that characterized by SEM. It suggests that the inner part of the microspheres is loose with large interspace. The large inner space will facilitate the drug-loading efficiency. From the low-magnification SEM images (Figure 2a,b), the $CoFe_2O_4$ porous microspheres show intact and uniform size. The energy-dispersive spectrometry (EDS) elemental mapping of the $CoFe_2O_4$ microspheres (Figure 3) confirms that the microspheres are a uniform distribution of Co, Fe, and O elements.

Figure 4 shows magnetic hysteresis loops for the $CoFe_2O_4$ porous microspheres. The magnetic hysteresis curves of the $CoFe_2O_4$ microspheres illustrate the strong magnetic response to a varying magnetic field. Their saturation magnetization is 62.4 emu/g, which is remarkably larger than that of the magnetic nanoparticles encapsulated with hollow mesoporous silica shells.[8−10] Combined with the inset picture, the magnetic

DOI: 10.1021/am507689a
ACS Appl. Mater. Interfaces 2015, 7, 1327−1333

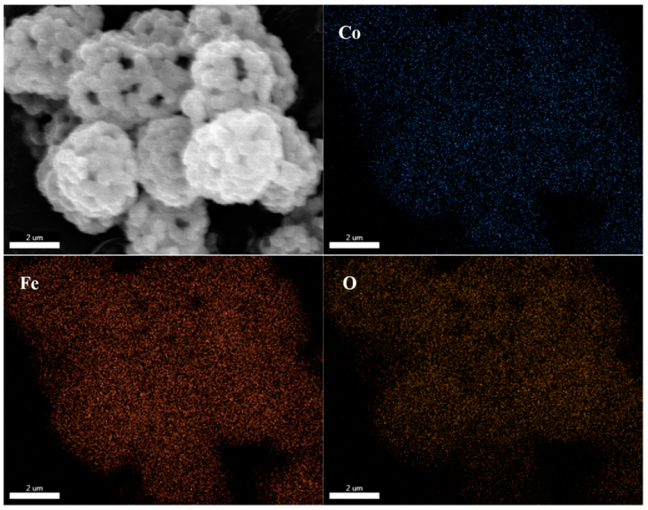

Figure 3. EDS elemental mapping of the $CoFe_2O_4$ microspheres.

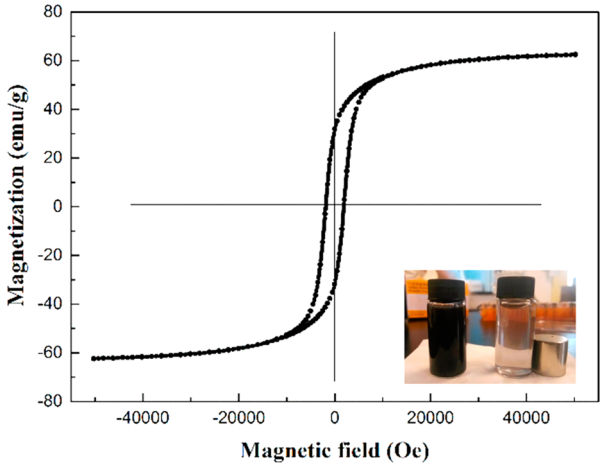

Figure 4. Magnetization curve of the $CoFe_2O_4$ microspheres. Inset: picture of the DOX-loaded nanocapsules and their response to an external magnet.

$CoFe_2O_4$ microspheres indicate excellent ability for magnetic guidance and drug release by application of a remote magnetic field.

3.2. Formation Mechanisms. To get more insight into the actual evolutionary process of $CoFe_2O_4$ porous microspheres, a series of time-dependent experiments were also performed in this work, and the intermediate products were thus sampled at different reaction stages (nucleation and growth, etc.). Figure 5 shows typical SEM images for the samples collected stepwise after 0.75, 1.5, 1.75, 2.25, and 20 h of reaction. These sequential images reveal a morphological evolution from nanoparticle aggregates to 3D hierarchical dandelion pollen grain structures. The crystal structure of partial intermediates intercepted at different reaction times was further investigated by XRD techniques (Figure 6). In the first stage of the hydrothermal reaction, the fast growth of a precursor generates nanoparticle aggregates, as shown in Figure 5a. Because Fe^{3+} can easily react with the OH^- produced by urea and NH_4F at relatively low pH, FeOOH is first formed after 45 min of reaction. On the basis of minimization of the Gibbs free energy, subsequent growth can take place around the grain boundary (Figure 5b,c). When the reaction time is increased, one can clearly see that the FeOOH grain gradually dissolved, which could be due to the instability

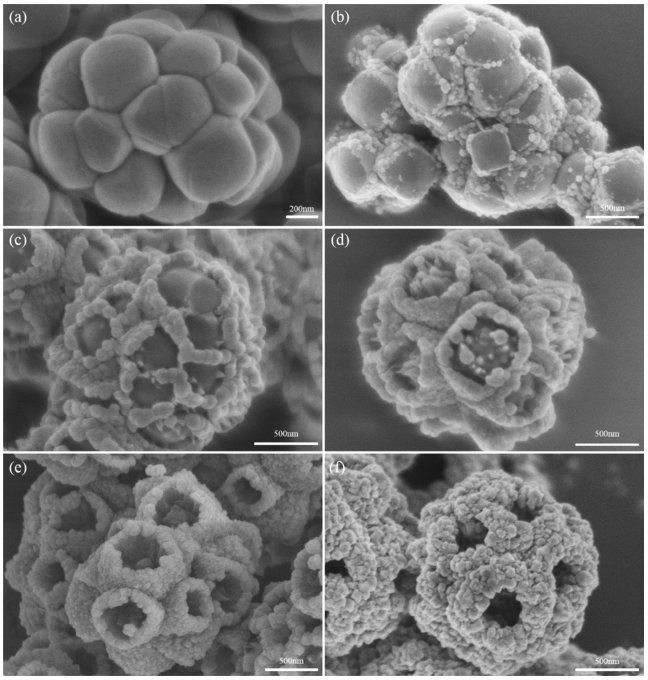

Figure 5. SEM image of the precursors synthesized at 180 °C for 0.75 (a), 1.5 (b and c), 1.75 (d), 2.25 (e), and 20 h (f).

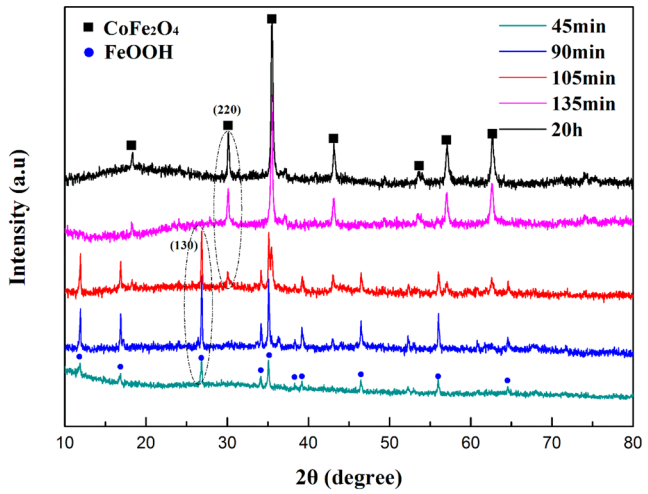

Figure 6. XRD pattern of the precursors synthesized at different times.

of the metastable phase in our present synthetic system. However, the dissolved Fe^{3+} combined with Co^{2+} can recrystallize into nanoparticles on the grain boundary to form a $CoFe_2O_4$ nanocomposite. When the reaction time increases to 20 h, 3D hierarchical $CoFe_2O_4$ porous microspheres are finally generated. It can be clearly seen from the XRD pattern (Figure 6) that FeOOH is first formed after 45 min of reaction, and the peaks of FeOOH gradually disappeared with the reaction time [such as (130) indexed in Figure 6]. Meanwhile, the peaks of $CoFe_2O_4$ gradually appeared [such as (220) indexed in Figure 6]. Finally, a pure $CoFe_2O_4$ XRD pattern is obtained after 20 h of reaction. It is confirmed that the start pH plays an important role in the formation of dandelion pollen-like morphology. A too high or too low pH value will lead to poor structure of $CoFe_2O_4$ (Figure S5 in the SI). It is because Fe^{3+} can easily hydrolyze at relatively low pH values. When the pH is too high, the hydrolysis of both Fe^{3+} and Co^{2+} will be

DOI: 10.1021/am507689a
ACS Appl. Mater. Interfaces 2015, 7, 1327−1333

very fast and too many nucleation sites are formed at the same time. The final morphology is just nanoparticles without specific morphology (Figure S5e,f in the SI). Also, with too low pH value, the hydrolysis of both Fe^{3+} and Co^{2+} can be suppressed and the reaction between Fe^{3+} and Co^{2+} gradually happens. The final morphology is also nanoparticles but with larger size and better crystallinity (Figure S5a,b in the SI). Only when pH is about 5, at this time, is the hydrolysis rate of both Fe^{3+} and Co^{2+} suitable, and the dandelion pollen-like morphology can be obtained. The in situ dissolution−recrystallization process[31] accompanied by morphology and phase change is clearly confirmed by the SEM image (Figure 5c−f) and XRD pattern (Figure 6). Our synthetic technique reveals that a novel crystal growth process for the fabrication of novel different complex micro/nanostructures can be achieved under the proper conditions.

3.3. Drug Loading and Release. To examine the potential of the prepared $CoFe_2O_4$ hollow porous microspheres for controlled drug delivery, DOX was first loaded into the nanocapsules, as illustrated in Scheme 1. Figure 7 shows the

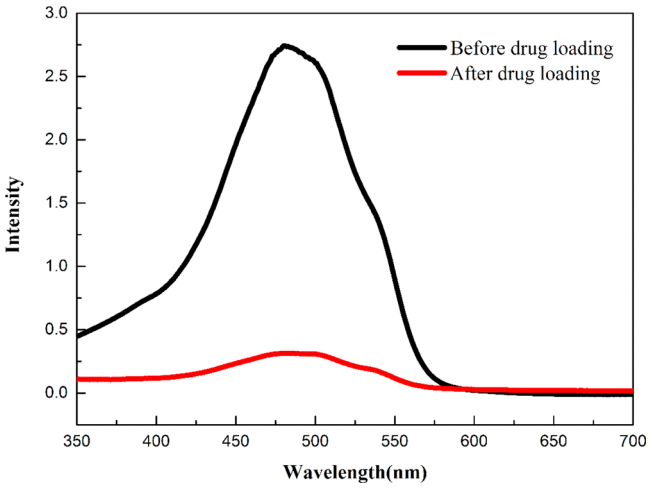

Figure 7. UV−vis absorption spectra of a DOX solution before and after loading in the $CoFe_2O_4$ microspheres.

UV−vis absorption spectra of a DOX solution before and after loading in the $CoFe_2O_4$ hollow porous microspheres. There is a significant reduction of the absorption intensity, indicating that the nanocapsules have good loading capacity. The loading efficiency of DOX is 88.6%, and the drug loading content is 118.1 mg of DOX/g of $CoFe_2O_4$ microspheres. The loading content is close to or even larger than the value of other magnetic nanoparticles (Table S1 in the SI). The large loading efficiency of DOX can be attributed to the large hollow interiors and electrostatic interaction between DOX and the $CoFe_2O_4$ porous spheres.

The drug-release profile from the DOX-loaded $CoFe_2O_4$ hollow porous microspheres was investigated in pH 7.4 and 5.0 buffer solutions at room temperature (Figure 8a). In both cases, DOX shows typical release profiles with a rapid release rate from the beginning, followed by a sustained release. The release behaviors agree with previously reported literature[32,33] because DOX is positively charged and $CoFe_2O_4$ is negatively charged in both pH 5 and 7.4 solutions, according to Figure S4 in the SI. However, the ζ potential of the $CoFe_2O_4$ microspheres at pH 7.4 is much lower than that at pH 5, which means that the electrostatic interaction decreases between DOX and $CoFe_2O_4$ at lower pH values. Hence, the release rate obviously increases when the pH is lowered. This observation suggests that the magnetic carriers containing a substantial amount of antitumor drugs can release more drugs in acidic tumor sites rather than normal tissues.

When an AMF was applied to the drug-loaded system, the drug-release property showed an obvious response to the magnetic field. Parts b−d of Figure 8 summarize the key results of this experiment, in which we measured the amount of the released drug depending on the external field strength and frequency. As a result, the AMF can significantly control the drug release. For comparison, the cumulative drug release under AMF exposure (200 Hz) is 54.6% within an 8 h window, which is much higher than the released amount without a magnetic field (29.5%). The data also confirm that, with higher frequency (Figure 8b,c) and magnetic field strength (Figure 8d), more DOX can be released from the system. However, the enhanced release gradually saturated after a frequency of 100 Hz. We suggest that the magnetic-enhanced drug release can contribute to the excellent magnetic properties and mechanical deformation that are triggered by its unique morphology. High magnetic properties can lead to thermal effects under AMF. As shown in Figure S1 in the SI, the room temperature is about 14.5 °C. When the AMF (200 Hz, 7.5 A) is applied, the temperature gradually increases and finally rises to 22.7 °C. A control experiment in which the solution containing the microspheres is simply heated without the applied field is set up. The temperature is controlled at 25 °C, a little higher than the equilibrium temperature with the applied field. It can be seen from Figure S2 in the SI that both the field-applied system and the simply heated system can lead to DOX release. However, the DOX-released efficiency of the field-applied system is higher than that of the simply heated system, which implies that our drug release system is due to not only the thermal effects but also the mechanical deformation that are triggered by its unique morphology as we proposed. What is more, we can see from Figure S3 in the SI that the morphology of the $CoFe_2O_4$ microspheres does not change much before and after drug release, indicating that the mechanical deformation is not destructive. The magnetic-controlled drug release is performed under a low-frequency magnetic field, indicating that the whole process has low energy consumption. Therefore, the $CoFe_2O_4$ hollow porous microspheres can be designed for controlled drug release by applying a remote magnetic field.

4. CONCLUSION

As a final remark, we have designed an effective route to synthesize 3D hierarchical $CoFe_2O_4$ porous microspheres, inspired by the morphology of dandelion pollen grains. It was found that the reaction time could sensitively affect the formation of $CoFe_2O_4$. More importantly, an in situ dissolution−recrystallization growth process is proposed, opening a new research opportunity for investigating the formation of novel micro/nanostructures. The obtained $CoFe_2O_4$ microsphere provides a large drug loading capacity and sustained release property. Furthermore, it shows excellent magnetic performance, which suggests good targeted-delivery capability of the designed drug carrier. The magnetic response of drug carriers with different magnetic frequencies and strengths can significantly promote the release of the loaded drug. It offers an additional feature that the controlled drug-release process can perform with a low-frequency AFM, which enables energy

DOI: 10.1021/am507689a
ACS Appl. Mater. Interfaces 2015, 7, 1327−1333

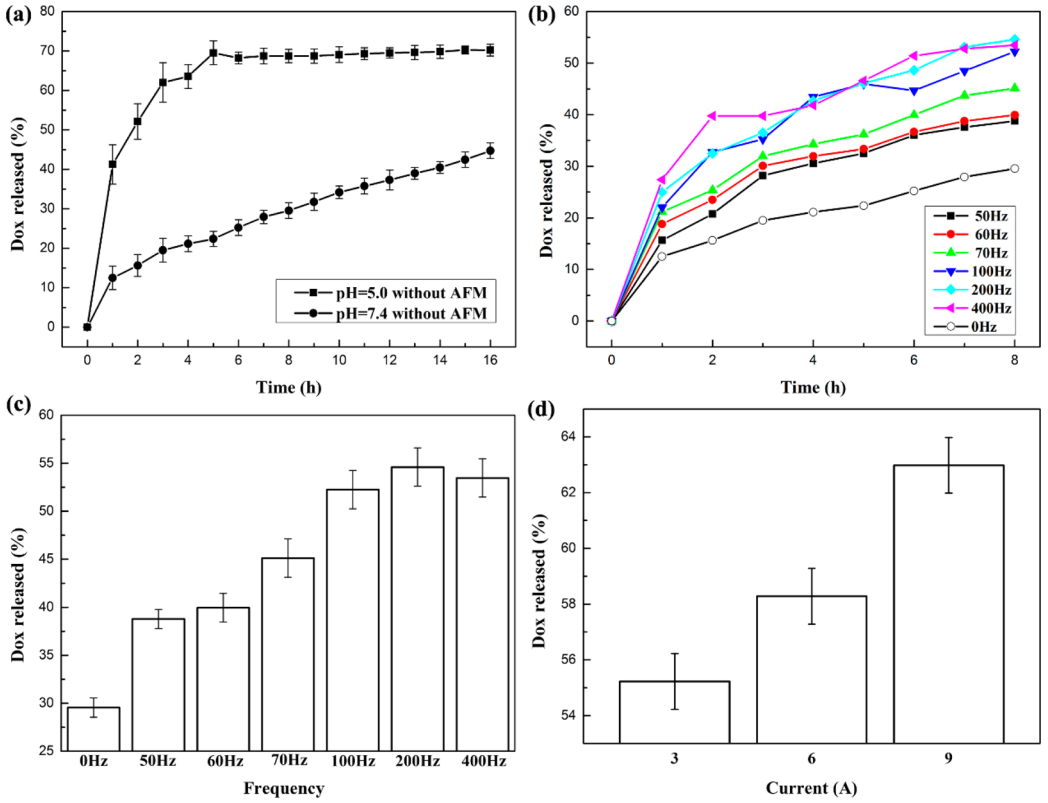

Figure 8. (a) Cumulative release of DOX at different pH values without AMF. Magnetically controlled DOX release under AFM with different frequencies (b and c) and strengths (d).

efficiency and environmental protection. Therefore, the 3D hierarchical $CoFe_2O_4$ porous microspheres proved to be promising materials for drug encapsulation and controlled drug-release applications.

■ ASSOCIATED CONTENT

Supporting Information

Description of the material and drug release. This material is available free of charge via the Internet at http://pubs.acs.org.

■ AUTHOR INFORMATION

Corresponding Author

*Tel: 0086-571-87952118. Fax: 0086-571-87952625. E-mail: huangjy@zju.edu.cn.

Notes

The authors declare no competing financial interest.

■ ACKNOWLEDGMENTS

This work was financially supported by the National Natural Science Foundation of China (Grant 91333203), Natural Science Foundation of Zhejiang province (Grant LY14E020006), and Doctorate Fund of the Ministry of Education (Grant 2011010110013).

■ REFERENCES

(1) Mura, S.; Nicolas, J.; Couvreur, P. Stimuli-Responsive Nanocarriers for Drug Delivery. *Nat. Mater.* **2013**, *12*, 991−1003.

(2) Horcajada, P.; Chalati, T.; Serre, C.; Gillet, B.; Sebrie, C.; Baati, T.; Eubank, J. F.; Heurtaux, D.; Clayette, P.; Kreuz, C. Porous Metal−Organic-Framework Nanoscale Carriers as a Potential Platform for Drug Delivery and Imaging. *Nat. Mater.* **2010**, *9*, 172−178.

(3) Chen, K.-J.; Liang, H.-F.; Chen, H.-L.; Wang, Y.; Cheng, P.-Y.; Liu, H.-L.; Xia, Y.; Sung, H.-W. A Thermoresponsive Bubble-Generating Liposomal System for Triggering Localized Extracellular Drug Delivery. *ACS Nano* **2012**, *7*, 438−446.

(4) Liu, Y.; Feng, L.; Liu, T.; Zhang, L.; Yao, Y.; Yu, D.; Wang, L.; Zhang, N. Multifunctional pH-Sensitive Polymeric Nanoparticles for Theranostics Evaluated in Experimental Cancer. *Nanoscale* **2013**, *6*, 3231−3242.

(5) Gui, R.; Wan, A.; Liu, X.; Jin, H. Intracellular Fluorescent Thermometry and Photothermal-Triggered Drug Release Developed from Gold Nanoclusters and Doxorubicin Dual-Loaded Liposomes. *Chem. Commun.* **2014**, *50*, 1546−1548.

(6) Schroeder, A.; Honen, R.; Turjeman, K.; Gabizon, A.; Kost, J.; Barenholz, Y. Ultrasound Triggered Release of Cisplatin from Liposomes in Murine Tumors. *J. Controlled Release* **2009**, *137*, 63−68.

(7) Hu, S.-H.; Chen, S.-Y.; Liu, D.-M.; Hsiao, C.-S. Core/Single-Crystal-Shell Nanospheres for Controlled Drug Release Via a Magnetically Triggered Rupturing Mechanism. *Adv. Mater.* **2008**, *20*, 2690−2695.

(8) Hu, S.-H.; Liu, D.-M.; Tung, W.-L.; Liao, C.-F.; Chen, S.-Y. Surfactant-Free, Self-Assembled PVA−Iron Oxide/Silica Core−Shell Nanocarriers for Highly Sensitive, Magnetically Controlled Drug Release and Ultrahigh Cancer Cell Uptake Efficiency. *Adv. Funct. Mater.* **2008**, *18*, 2946−2955.

(9) Zhu, Y.; Fang, Y.; Kaskel, S. Folate-Conjugated Fe_3O_4@SiO_2 Hollow Mesoporous Spheres for Targeted Anticancer Drug Delivery. *J. Phys. Chem. C* **2010**, *114*, 16382−16388.

(10) Zhu, Y.; Ikoma, T.; Hanagata, N.; Kaskel, S. Rattle-Type Fe_3O_4@SiO_2 Hollow Mesoporous Spheres as Carriers for Drug Delivery. *Small* **2010**, *6*, 471−478.

(11) Lu, F.; Popa, A.; Zhou, S.; Zhu, J.-J.; Samia, A. C. S. Iron Oxide-Loaded Hollow Mesoporous Silica Nanocapsules for Controlled Drug Release and Hyperthermia. *Chem. Commun.* **2013**, *49*, 11436−11438.

DOI: 10.1021/am507689a
ACS Appl. Mater. Interfaces 2015, 7, 1327−1333

(12) Sun, Y.; Ji, G.; Zheng, M.; Chang, X.; Li, S.; Zhang, Y. Synthesis and Magnetic Properties of Crystalline Mesoporous $CoFe_2O_4$ with Large Specific Surface Area. *J. Mater. Chem.* **2010**, *20*, 945−952.
(13) Mohapatra, S.; Rout, S. R.; Maiti, S.; Maiti, T. K.; Panda, A. B. Monodisperse Mesoporous Cobalt Ferrite Nanoparticles: Synthesis and Application in Targeted Delivery of Antitumor Drugs. *J. Mater. Chem.* **2011**, *21*, 9185−9193.
(14) Nidhin, M.; Nazeer, S. S.; Jayasree, R. S.; Kiran, M. S.; Nair, B. U.; Sreeram, K. J. Flower Shaped Assembly of Cobalt Ferrite Nanoparticles: Application as T-2 Contrast Agent in Mri. *RSC Adv.* **2013**, *3*, 6906−6912.
(15) Zavaliche, F.; Zhao, T.; Zheng, H.; Straub, F.; Cruz, M.; Yang, P.-L.; Hao, D.; Ramesh, R. Electrically Assisted Magnetic Recording in Multiferroic Nanostructures. *Nano Lett.* **2007**, *7*, 1586−1590.
(16) Tang, D.; Yuan, R.; Chai, Y.; An, H. Magnetic-Core/Porous-Shell $CoFe_2O_4/SiO_2$ Composite Nanoparticles as Immobilized Affinity Supports for Clinical Immunoassays. *Adv. Funct. Mater.* **2007**, *17*, 976−982.
(17) Yang, X.; Wang, X.; Zhang, Z. Electrochemical Properties of Submicron Cobalt Ferrite Spinel through a Co-Precipitation Method. *J. Cryst. Growth* **2005**, *277*, 467−470.
(18) Li, X.-H.; Xu, C.-L.; Han, X.-H.; Qiao, L.; Wang, T.; Li, F.-S. Synthesis and Magnetic Properties of Nearly Monodisperse $CoFe_2O_4$ Nanoparticles through a Simple Hydrothermal Condition. *Nanoscale Res. Lett.* **2010**, *5*, 1039−1044.
(19) Cannas, C.; Musinu, A.; Peddis, D.; Piccaluga, G. Synthesis and Characterization of $CoFe_2O_4$ Nanoparticles Dispersed in a Silica Matrix by a Sol−Gel Autocombustion Method. *Chem. Mater.* **2006**, *18*, 3835−3842.
(20) Hall, S. R.; Swinerd, V. M.; Newby, F. N.; Collins, A. M.; Mann, S. Fabrication of Porous Titania (Brookite) Microparticles with Complex Morphology by Sol−Gel Replication of Pollen Grains. *Chem. Mater.* **2006**, *18*, 598−600.
(21) Song, F.; Su, H.; Han, J.; Lau, W. M.; Moon, W.-J.; Zhang, D. Bioinspired Hierarchical Tin Oxide Scaffolds for Enhanced Gas Sensing Properties. *J. Phys. Chem. C* **2012**, *116*, 10274−10281.
(22) Yang, F.; Su, H.; Zhu, Y.; Chen, J.; Lau, W. M.; Zhang, D. Bioinspired Synthesis and Gas-Sensing Performance of Porous Hierarchical A-Fe_2O_3/C Nanocomposites. *Scr. Mater.* **2013**, *68*, 873−876.
(23) Hall, S. R.; Bolger, H.; Mann, S. Morphosynthesis of Complex Inorganic Forms Using Pollen Grain Templates. *Chem. Commun.* **2003**, 2784−2785.
(24) Kulak, A.; Hall, S. R.; Mann, S. Single-Step Fabrication of Drug-Encapsulated Inorganic Microspheres with Complex Form by Sonication-Induced Nanoparticle Assembly. *Chem. Commun.* **2004**, 576−577.
(25) Fu, M.; Jiao, Q.; Zhao, Y.; Li, H. Vapor Diffusion Synthesis of $CoFe_2O_4$ Hollow Sphere/Graphene Composites as Absorbing Materials. *J. Mater. Chem. A* **2014**, *2*, 735−744.
(26) Zhou, Z.; Zhang, Y.; Wang, Z.; Wei, W.; Tang, W.; Shi, J.; Xiong, R. Electronic Structure Studies of the Spinel $CoFe_2O_4$ by X-Ray Photoelectron Spectroscopy. *Appl. Surf. Sci.* **2008**, *254*, 6972−6975.
(27) Meng, Y.; Chen, D.; Jiao, X. Synthesis and Characterization of $CoFe_2O_4$ Hollow Spheres. *Eur. J. Inorg. Chem.* **2008**, *2008*, 4019−4023.
(28) Qi, Z.; Gong, Y.; Zhang, C.; Xu, J.; Wang, X.; Zhao, C.; Ji, H.; Zhang, Z. Fabrication and Characterization of Magnetic Nanoporous Cu/$(Fe,Cu)_3O_4$ Composites with Excellent Electrical Conductivity by One-Step Dealloying. *J. Mater. Chem.* **2011**, *21*, 9716−9724.
(29) Zhu, J.; Gu, H.; Guo, J.; Chen, M.; Wei, H.; Luo, Z.; Colorado, H. A.; Yerra, N.; Ding, D.; Ho, T. C. Mesoporous Magnetic Carbon Nanocomposite Fabrics for Highly Efficient Cr (Vi) Removal. *J. Mater. Chem. A* **2014**, *2*, 2256−2265.
(30) Zhang, X.; Zhu, Y.; Yang, X.; Zhou, Y.; Yao, Y.; Li, C. Multifunctional Fe_3O_4@TiO_2@Au Magnetic Microspheres as Recyclable Substrates for Surface-Enhanced Raman Scattering. *Nanoscale* **2014**, *6*, 5971−5979.
(31) Bai, J.; Li, X.; Liu, G.; Qian, Y.; Xiong, S. Unusual Formation of $ZnCo_2O_4$ 3d Hierarchical Twin Microspheres as a High-Rate and Ultralong-Life Lithium-Ion Battery Anode Material. *Adv. Funct. Mater.* **2014**, *24*, 3012−3020.
(32) Chang, B.; Sha, X.; Guo, J.; Jiao, Y.; Wang, C.; Yang, W. Thermo and pH Dual Responsive, Polymer Shell Coated, Magnetic Mesoporous Silica Nanoparticles for Controlled Drug Release. *J. Mater. Chem.* **2011**, *21*, 9239−9247.
(33) Muhammad, F.; Guo, M.; Qi, W.; Sun, F.; Wang, A.; Guo, Y.; Zhu, G. pH-Triggered Controlled Drug Release from Mesoporous Silica Nanoparticles Via Intracelluar Dissolution of ZNO Nanolids. *J. Am. Chem. Soc.* **2011**, *133*, 8778−8781.

DOI: 10.1021/am507689a
ACS Appl. Mater. Interfaces 2015, 7, 1327−1333